Available online at www.sciencedirect.com
SCIENCE DIRECT
Journal of Solid State Chemistry 179 (2006) 1957–1964
JOURNAL OF SOLID STATE CHEMISTRY
www.elsevier.com/locate/jssc

Substitution clustering in a non-stoichiometric celsian synthesized by the thermal transformation of barium exchanged zeolite X

Nigel J. Clayden[a,*], Serena Esposito[b], Claudio Ferone[b], Michele Pansini[b]

[a]School of Chemical Sciences and Pharmacy, University of East Anglia, NR4 7TJ, UK
[b]Laboratorio Materiali del Dipartimento di Meccanica, Strutture, Ambiente e Territorio, Facoltà di Ingegneria dell'Università di Cassino, Via G. Di Biasio 43, 03043 Cassino (FR), Italy

Received 20 January 2006; received in revised form 23 February 2006; accepted 11 March 2006
Available online 24 March 2006

Abstract

The thermal transformation of Ba exchanged zeolite X to celsian has been studied by ^{27}Al and ^{29}Si MAS NMR spectroscopy. Evidence for the degradation of the zeolite framework is present in the ^{29}Si NMR spectra after thermal treatment at 850 °C. Confirmation is provided by the ^{29}Si NMR data that synthesis of celsian via the decomposition of Ba exchanged zeolite leads to a single defect phase. Clustering of the isomorphous replacement of aluminium by silicon must occur to explain the observed ^{29}Si chemical shifts. The ^{27}Al NMR data show distorted aluminium co-ordination sites upon the thermal transformation of Ba exchanged zeolite X. The distortions present in the amorphous matrix are greater than those present in the monoclinic and hexagonal crystalline phases of celsian.

Keywords: Zeolite X; Non-stoichiometric celsian; ^{27}Al MAS NMR; ^{29}Si MAS NMR

1. Introduction

Non-traditional applications of zeolites include their use as starting materials for the synthesis of advanced ceramics [1–4]. The advantages of this technique are threefold. First the versatility of the zeolite structure in terms of the Si/Al ratio [5–7] and the possibility of cation exchange means that a starting material of the desired composition can always be made. Secondly, the amorphous phase arising from the thermal collapse of the microporous zeolite structure exhibits a perfect compositional homogeneity at an atomic scale. Thirdly, zeolites represent low cost starting materials. A much studied system has been the thermal transformations of Ba-exchanged zeolites into monoclinic celsian ($BaAl_2Si_2O_8$) [8–17] in large part because of the excellent technological properties of this ceramic phase: such as high melting point, low thermal expansion coefficient up to about 1000 °C, absence of phase transitions up to 1590 °C, low dielectric constant, and low dielectric loss [18], coupled with the considerable problems arising in its synthesis.

One aspect, which has not been considered in detail, is the consequence of the thermal transformation of a starting zeolite, which does not properly reproduce the desired composition of the celsian phase. Previous work has shown that celsian is the only ternary phase in the $BaO–Al_2O_3–SiO_2$ phase diagram [19] consequently either a non-stoichiometric form of the desired phase [20,21] must be formed or the stoichiometric phase together with another binary or single possibly glassy phase. When a non-stoichiometric phase is formed two questions arise: First, the extent to which an excess of silica can be accommodated and second whether the distribution of silicon and aluminium across the T sites in the parent zeolite is preserved. Judging by the accidental synthesis of $Ba_{0.8}Al_{11.6}Si_{2.4}O_8$ an Si/Al ratio of up to 1.5 can be tolerated [22], though whether this is possible via a zeolite precursor remains an open question. The evidence presented concerning the distribution of Si and Al is ambiguous. For the non-stoichiometric celsian above complete Si and Al disorder was deduced from the single crystal X-ray data but this cannot be related to a parent zeolite since no

*Corresponding author. Fax: +44 1603 592003.
E-mail address: N.Clayden@uea.ac.uk (N.J. Clayden).

0022-4596/$ - see front matter © 2006 Elsevier Inc. All rights reserved.
doi:10.1016/j.jssc.2006.03.021

zeolite was used in its synthesis. In the case of a non-stoichiometric celsian prepared from Ba exchanged faujasite ^{29}Si NMR results again indicate a disordered distribution of Si and Al in the T sites [20], but the relative intensities of the $Q_4(m\mathrm{Al})$ resonances do not appear to be consistent with the stated Si/Al ratio of 1.33 obtained from a chemical analysis of the product. Indeed, a crude estimate based on the relative peak heights, which is independent of the presence of ordering, suggests an Si/Al ratio of 1.12. Furthermore ^{29}Si NMR data were not presented for the starting zeolite.

In the present paper we report ^{29}Si NMR evidence for the formation of a non-stoichiometric celsian from Ba exchanged X zeolite in the presence of a significant excess of silicon which does not preserve the Si and Al distribution seen in the original zeolite.

2. Experimental section

Carlo Erba reagent-grade synthetic zeolite 13X was used. A second zeolite X composition was synthesised in laboratory starting from a synthesis batch of the following composition: $5.5Na_2O{:}1.65K_2O{:}2.2SiO_2{:}1Al_2O_3{:}122H_2O$. This batch was obtained according to the following procedure: (1) Reagent grade Riedel-de-Haen hydrate alumina (Al_2O_3 65%) was dissolved in a NaOH solution prepared by dissolving reagent grade Carlo Erba NaOH in doubly distilled water. (2) Reagent grade Carlo Erba KOH was added to this solution. (3) Reagent grade BHD sodium silicate aqueous solution (SiO_2: 27.5%, Na_2O 8.0%) was added to this solution. This batch was kept at 70 °C for 3 h and then at 95 °C for 2 h under autogeneous pressure and continuous stirring. The final product was recovered by vacuum filtration, abundantly washed with doubly distilled water, dried at 75 °C for 24 h and stored for at least 3 days in an environment having about 50% relative humidity to allow water saturation. These materials will be identified from this point onward as zeolites Na-X and (Na, K)-X, respectively.

These zeolites were subjected to exhaustive Ba-exchange. Exchange operations, which were terminated when their iteration did not give rise to a sensible decrease of the alkaline cations residual amount, were performed as follows.

Zeolite Na-X was contacted with a warm (60–70 °C) $[Ba^{2+}] = 0.5$ N solution with a weight solid/liquid ratio (S/L) = 1/25. The solution was prepared using doubly distilled water and Carlo Erba reagent-grade $Ba(NO_3)_2$ (purity 99.5%). The solid was separated from the liquid through filtration and again contacted with the exchange solution for a total of four times. Then a fifth exchange was performed using a $[Ba^{2+}] = 0.2$ N solution, all other conditions being equal to previous ones.

Zeolite (Na, K)-X was contacted with a warm (60–70 °C) $[Ba^{2+}] = 0.2$ N solution with a weight solid/liquid ratio (S/L) = 1/25. The solution was prepared using doubly distilled water and Carlo Erba reagent-grade $Ba(NO_3)_2$ (purity 99.5%). The solid was separated from the liquid through filtration and again contacted with the exchange solution for a total of seven times.

The length of each exchange ranged between 12 and 18 h and the initial pH of Ba^{2+} solutions used for the exchanges was about 5.8. The materials obtained according to these procedures will be identified from this point onward as zeolites Ba-X, I and II, respectively. These Ba-exchanged zeolite samples were washed with doubly distilled water, dried for about 1 day at 80 °C and stored for at least 3 days in an environment having about 50% relative humidity to allow water saturation of zeolites. Then the zeolites Ba-X I and II were subjected to complete chemical analysis using the procedure described in Ref. [13], from which the following chemical formulas were calculated:

$$\text{Ba I} = Ba_{39.69}Na_{1.62}Al_{81}Si_{111}O_{384}250H_2O\ \mathrm{Si/Al} = 1.36,$$

$$\text{Ba II} = Ba_{42.14}Na_{1.53}K_{0.17}Al_{86}Si_{106}O_{384}243H_2O\ \mathrm{Si/Al0} = 1.23$$

Ba-exchanged zeolite X samples, obtained following the above procedures, were subjected to the following thermal treatments: 2 h at 850 °C, 1 h at 1000 °C and 28 h at 1200 °C. A Lenton furnace, which ensures stable temperature to within ±2 °C, and Al_2O_3 crucibles were used. The samples were heated at a rate of 10 °C/min up to the fixed temperature, kept in this condition for the fixed time, and subsequently cooled in air.

These products were characterised by X-ray diffraction (XRD) at room temperature using a Philips X'PERT diffractometer, Cu$K\alpha$ radiation, collection of data between 20° and 40° 2θ with a step width of 0.02° 2θ and 1 s data collection per step.

Solid-state ^{27}Al MAS NMR data, were acquired at 14.07 T (156.37 MHz) using a Chemagnetics 600 spectrometer and a 4 mm Doty high-speed MAS probe spun at 10–12 kHz. Data acquisition conditions were a 0.5 μs, 15° pulse and a recycle time of 1 s over a spectral window of 1 MHz collecting typically of the order of 1000 transients. The spectra were referenced against $Y_3Al_5O_{12}$ at 0.7 ppm (with respect to a primary shift scale reference of $Al(H_2O)_6^{3+}$ at 0.000 ppm). ^{29}Si MAS NMR data were acquired at 4.7 T (39.7 MHz) using a Bruker MSL 200 NMR spectrometer and a 7 mm standard MAS probe spun at 4 kHz. Data acquisition conditions were a 5 μs, 90° pulse with a recycle time of 60 s over a spectral window of 20 kHz, collecting of the order of 1000 transients. Spectra were referenced against Q_8M_8 at +11.5 ppm (with respect to the primary shift scale reference of TMS at 0.000 ppm).

Monte Carlo calculations of the $Q_4(m\mathrm{Al})$ intensities were based on method described in Ref. [23]. A three dimensional grid of 100 × 100 × 2 together with periodic boundary conditions was used to represent the double layer structural element of α-hexagonal celsian [24]. Si or Al atoms were initially placed randomly on the grid. Subsequently atom pairs were chosen at random and swapped to minimise the total number of Al–Al nearest neighbours, thereby obeying Lowensteins Rule. At Si/Al ratios close to

1.0 the elimination of all Al–Al contacts became very slow requiring in excess of 10^8 swaps.

3. Results

The X-ray diffraction patterns of zeolite X I sample are reported in Fig. 1. In particular curve a represents the XRD pattern of zeolite X I sample in its original composition (Na form) and curve b after Ba-exchange. Curves c, d and e refer to the Ba-exchanged zeolite X I sample thermally treated at 850 °C for 2 h, 1000 °C for 1 h and 1200 °C for 28 h, respectively. Curve c is indicative of a completely amorphous system. In Ba-exchanged zeolite X I sample thermally treated at 1000 °C for 1 h (curve d) the only crystalline phase present is hexacelsian, whereas in Ba-exchanged zeolite X I sample thermally treated at 1200 °C for 28 h (curve e) a considerable amount of hexacelsian together with a small amount of monoclinic celsian were the only crystalline phases that could be detected. In curves d and e only the main diffraction peaks of hexacelsian and monoclinic celsian are labelled with the letters H and M, respectively. XRD patterns of homologous samples of zeolite X II are not reported in as much as they closely resemble those of zeolite X I, the exception being the presence of diffraction peaks of zeolite A impurity. The ^{29}Si MAS NMR spectra for the zeolite X I are shown in Fig. 2 while the ^{29}Si and ^{27}Al NMR data for zeolite X II are available as Supplementary Information. A comparison of the Ba^{2+} exchanged zeolite X and the derived celsian is shown in Fig. 3. The variation in the $Q_4(m\mathrm{Al})$ intensities in the ^{29}Si MAS NMR spectrum as a function of the aluminium mole fraction is shown in Fig. 4. The ^{27}Al MAS NMR spectra of zeolite X I are shown in Fig. 5. Only the central transition lines of the ^{27}Al NMR spectra are shown, full spectral width data showing the spinning sideband manifold are available as Supplementary Information.

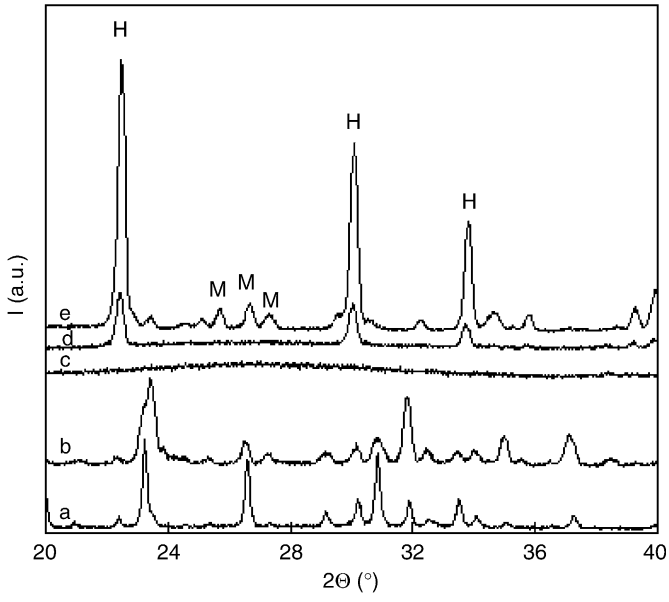

Fig. 1. X-ray diffraction patterns of zeolite X (a) Initial (b) After Ba-exchange (c) After heating to 850 °C for 2 h and (d) After heating to 1000 °C for 1 h and (e) After heating to 1200 °C for 28 h. H, hexagonal and M, monoclinic celsian.

4. Discussion

4.1. ^{29}Si NMR

Before a detailed consideration of the spectra is made it is perhaps worth noting at the outset the remarkable similarity in the spectral data for the two X compositions, demonstrating the reproducibility in the structural changes. At the level of the short range ordering seen by solid state NMR there is essentially no difference in the thermal transformations though there are subtle difference seen in the ^{29}Si NMR spectra around −105 ppm associated with $Q_4(0\mathrm{Al})$. Looking at the ^{29}Si NMR spectra, the characteristic feature of the ^{29}Si NMR spectrum of zeolites and aluminosilicates is the pattern of resonances associated with the nearest neighbours as exemplified by the $Q_n(m\mathrm{Al})$ connectivity [25]. Cation effects have a secondary effect on the ^{29}Si chemical shifts, and whilst profound changes can be seen with the SiOX bond angle, in particular when the Si–O–Si bond angle approaches 180°, by and large the range in chemical shifts is small. Thus NMR chemical shifts are sensitive to very local effects, 3–4 Å and more distant effects caused by changes in bond angles and atom connectivity in the next nearest neighbours are generally reflected in changes lying within the natural linewidths. This is especially true in disordered materials where a range of such variations leads to broad lines.

For Na-X the ^{29}Si MAS NMR spectrum is consistent with the literature with the pattern of resonances reflecting $Q_4(m\mathrm{Al})$ with Si/Al > 1.0.[25] When Si/Al = 1.0 and with strict adherence to Lowenstein's rule a single resonance is expected at $Q_4(4\mathrm{Al})$ $\delta = -85$ ppm. Analysis of the ^{29}Si NMR spectra by fitting the resonances to a series of Gaussian functions yields Si/Al ratios similar to those obtained by chemical analysis, for Na-X Si/Al = 1.29 and for (Na,K)-X Si/Al = 1.25. Upon exchange with barium the resonances broaden showing that the barium must be perturbing the order, though, in contrast to zeolite A [16], the broadening is less and the crystallinity better preserved. Although the resolution of distinct $Q_4(m\mathrm{Al})$ resonances is lost the overall lineshape appears to reflect that seen for Na-X, suggesting the maintenance of the longer range order. Substitution of Na^+ by Ba^{2+} has little effect on the ^{29}Si chemical shift. Heating the Ba-exchanged zeolite X I to 850 °C leads to a much broader resonance and the loss of all fine structure, consistent with a fully amorphous material. With further heating of the Ba-exchanged zeolite X I to 1000 °C, a temperature at which hexagonal celsian is seen in the powder XRD, the resonance sharpens, consistent with the formation of an ordered structure, at the chemical shift expected for hexagonal celsian. Although powder XRD also shows a small monoclinic component,

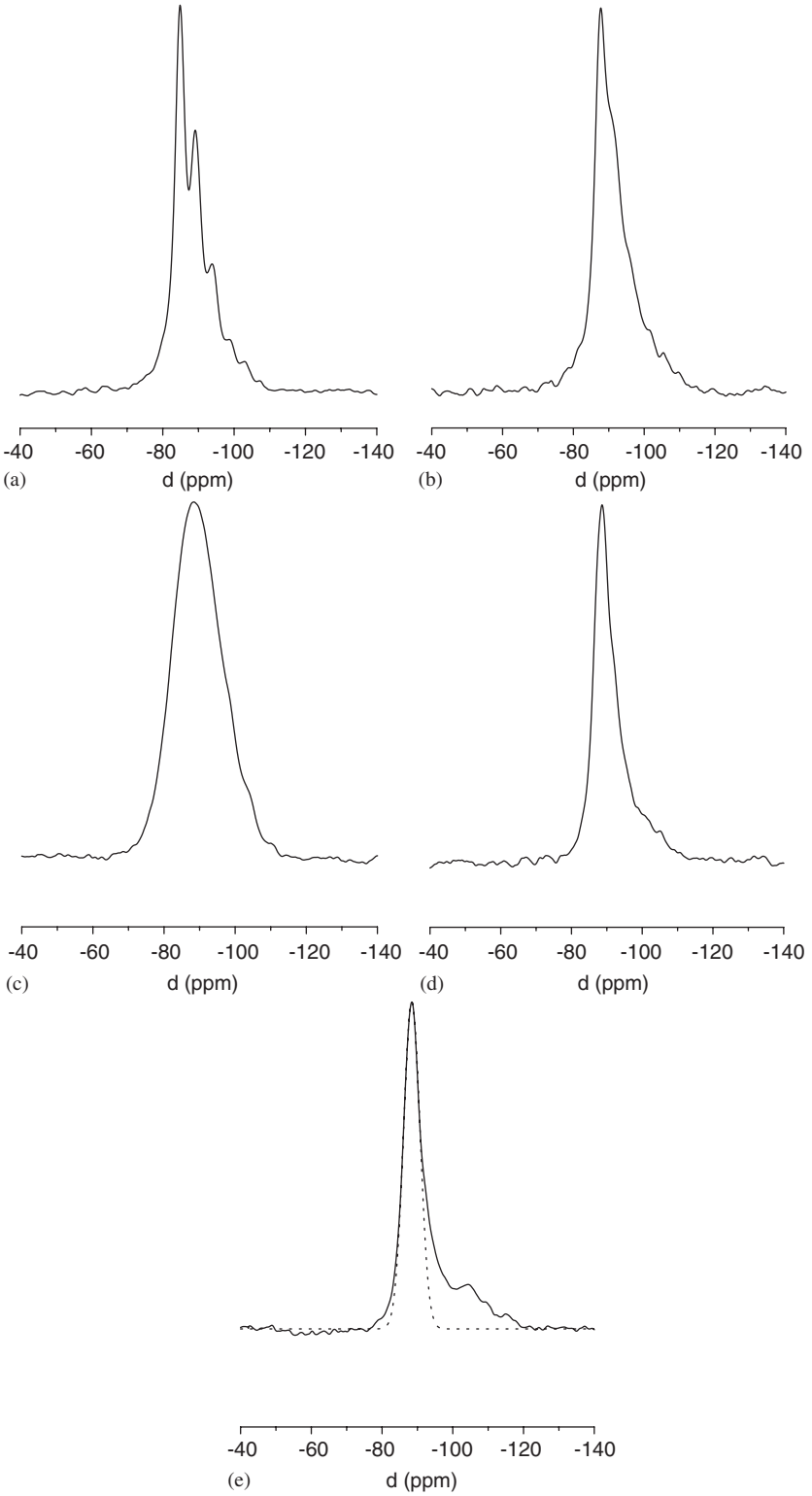

Fig. 2. ^{29}Si MAS NMR spectra at 39.73 MHz of zeolite X I, (a) Initial (b) After Ba-exchange (c) After heating to 850 °C for 2 h and (d) After heating to 1000 °C for 1 h and (e) After heating to 1200 °C for 28 h. The dotted line shows a gaussian fit to the deshielded side of the resonance at −88.2 ppm.

this cannot be resolved. In addition the resonance associated with celsian shows a significant tailing on the more shielded side. For a stoichiometric celsian a symmetric gaussian lineshape is expected [26]. Three explanations for the tailing are possible. First incomplete crystallisation from the disordered post zeolite structure evident in the ^{29}Si NMR spectrum of the 850 °C sample. Second, $Q_4(m\mathrm{Al})$ $m = 3, 2, 1, 0$ sites arising from a non-stoichiometric celsian and thirdly the presence of an unidentified glassy aluminosilicate phase. On further

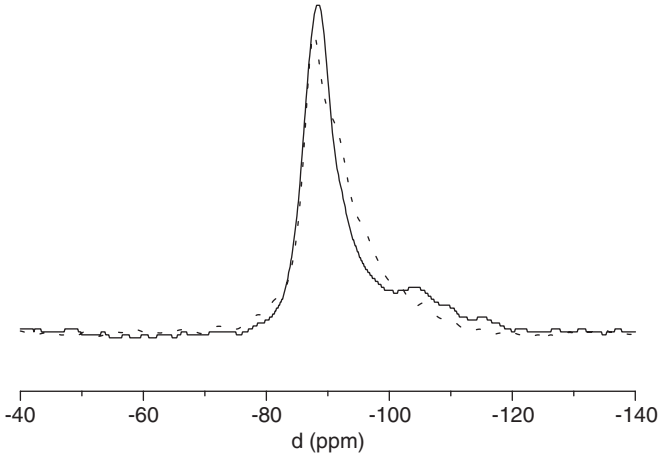

Fig. 3. Comparison ^{29}Si MAS NMR spectra at 39.73 MHz of zeolite X after Ba exchange(solid line) and after heating to 1200 °C for 28 h (dotted line). Spectra are normalised to the same total integral.

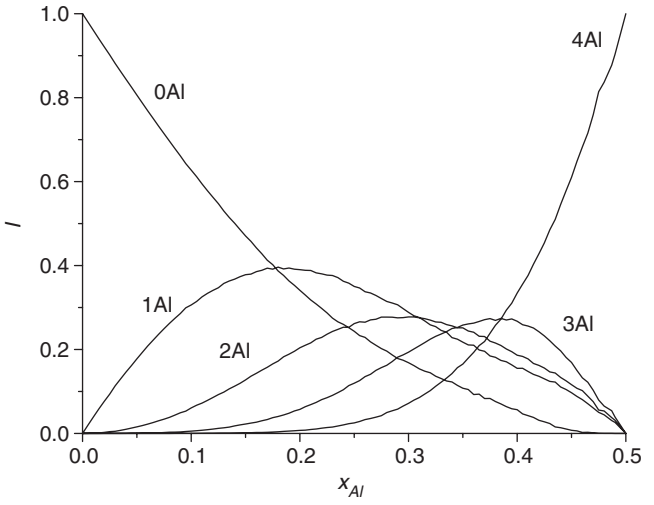

Fig. 4. Monte Carlo calculated ^{29}Si NMR peak intensities for α-hexagonal celsian assuming a random Al distribution obeying Lowenstein's Rule as a function of the mole fraction of Al.

heating to 1200 °C the resonance at ca. −88 ppm narrows further indicative of a more ordered structure. Despite this narrowing the tailing remains at the same intensity and indeed becomes better defined with clearer evidence for a number of resonance. Accurate modelling of the intensity in terms of different sites, however, is not possible because of a lack of resolution although a symmetric gaussian lineshape calculated by fitting the deshielded side of the resonance has been included in Fig. 2e to highlight the tailing. Importantly because the tailing is not reduced by the additional heat treatment it is unlikely to be caused by residual disordered phases arising from the breakdown of the zeolite structure.

As noted in the Introduction an alternative mechanism by which a silicon excess can be accommodated is by the formation of an amorphous phase, which in the case of a silicon excess most plausibly is a glassy silica. However, the extensive chemical shift range for the ^{29}Si not associated with a stoichiometric celsian categorically rules out amorphous silica as the sole origin of this tailing, although the presence of some cannot be ruled out. Barium silicate phases can be ruled out because the starting zeolite is intrinsically barium deficient. Although the formation of an unidentified aluminosilicate phase cannot be entirely ruled out, the ^{27}Al NMR spectra described in the following section, argue against the presence of any such phases. In particular the absence of minor resonances corresponding to tetrahedral aluminium, the symmetric nature of the observed resonance at 60.3 ppm and the close similarity in the spectra with earlier ones for a hexagonal celsian standard [16]. The assignment of the resonance intensity in the region −95 ppm to −120 ppm to $Q_4(m\mathrm{Al})$ $m = 3,2,1,0$ sites within a non-stoichiometric celsian is exactly analogous to the precursor zeolite X. Thus, in a stoichiometric celsian with $\mathrm{Si/Al} = 1$ the operation of Lowensteins rule results in complete ordering within the aluminosilicate framework,leading to only $Q_4(4\mathrm{Al})$ resonances. On the other hand for a non-stoichiometric celsian, $\mathrm{Ba}_{(1-x)}\square_x\mathrm{Al}_{(2-2x)}\mathrm{Si}_{(2+2x)}\mathrm{O}_8$, where isomorphous substitution of Al by Si takes place in the aluminosilicate framework a range of $Q_4(m\mathrm{Al})$ $m = 3,2,1,0$ co-ordinations become possible together with Ba vacancies, □, to compensate for the excess of positive electrical charge [20,21].

Moreover, if the Si and Al disorder across the T sites is the same in the resulting non-stoichiometric celsian as the parent zeolite the pattern of intensities in the ^{29}Si NMR spectrum must also be the same. Confirmation of this statement is provided by the Monte Carlo computer calculations. Although small differences are seen in the intensities of the $Q_4(m\mathrm{Al})$ resonances as a function of the mole fraction of aluminum compared to those seen for zeolite X overall they mirror the intensities shown in Fig. 4 of Ref. [23]. The Si/Al ratio for the two zeolites used in the present study correspond to $x_{\mathrm{Al}} = 0.423$–0.448. Anchoring the set of chemical shifts corresponding to the $Q_4(m\mathrm{Al})$ sites in a non-stoichiometric celsian is straightforward since the ^{29}Si chemical shifts for the $Q_4(4\mathrm{Al})$ units in hexagonal celsian (−88.2 ppm), Ba-X I(−87.8 ppm) and Ba-X II(−88.9 ppm) are much the same. Thus the ranges seen for the parent Ba exchanged zeolites are applicable. In effect if the Si, Al disorder present in the parent zeolite is preserved in the non-stoichiometric celsian then very similar ^{29}Si NMR spectra for the precursor zeolite and product celsian are expected. This is not seen in the present case, and although the differences are quite subtle, Fig. 3, the reduced intensity in the $Q_4(3\mathrm{Al})$ and $Q_4(2\mathrm{Al})$ resonances and the greater intensity in the $Q_4(0\mathrm{Al})$ region than predicted, both suggest a clustering of the Si substitutions.

Turning now to the X II zeolite, only two differences from the X I zeolite series are apparent in the ^{29}Si NMR spectra. First, the initial spectrum shows a lower intensity in the more shielded resonances as expected for a Si/Al ratio closer to 1. Second, the intensity of the resonance assigned to a substitution defect is lower, consistent with the smaller silicon excess in the X II zeolite. Apart from

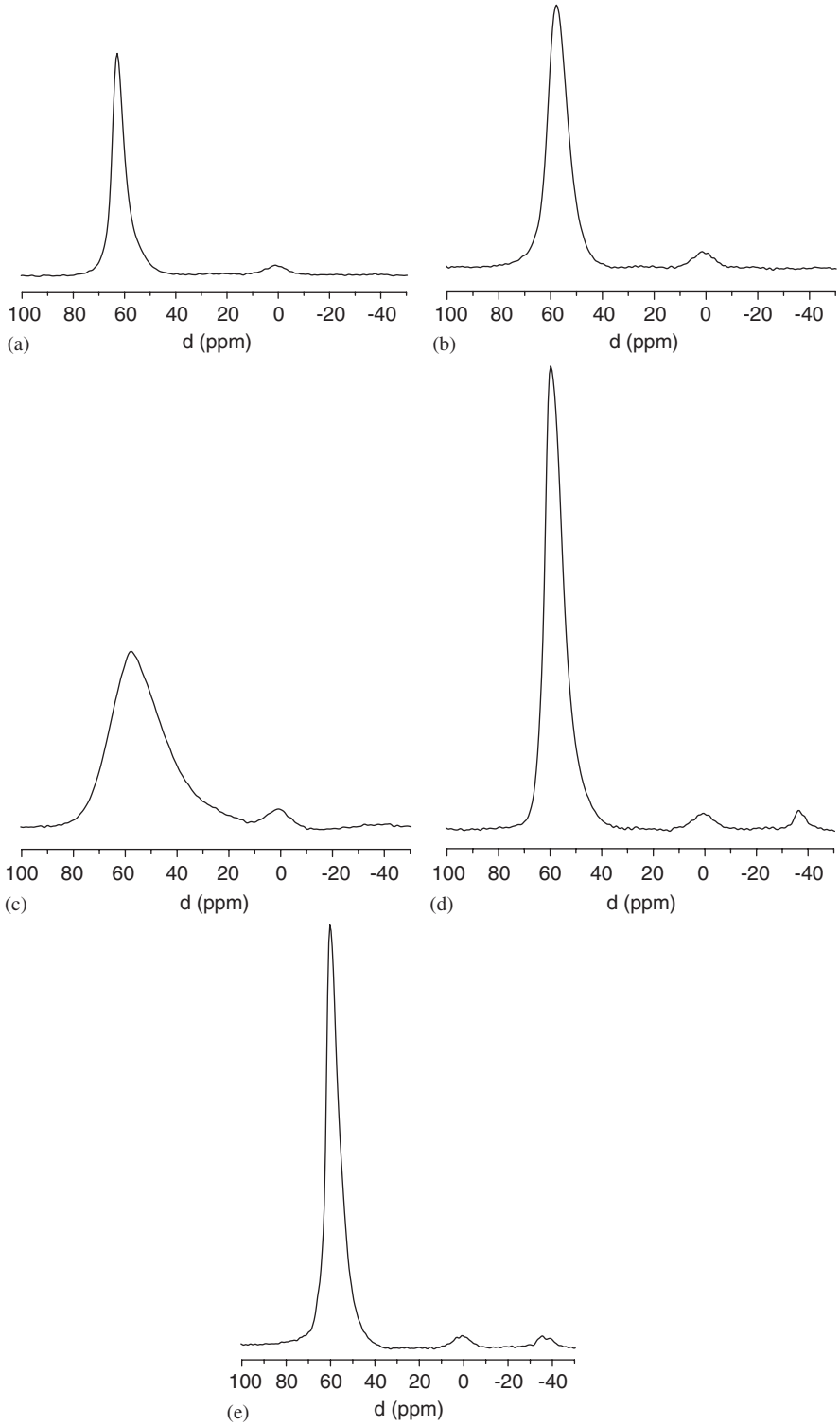

Fig. 5. ^{27}Al MAS NMR spectra at 156.37 MHz of zeolite X I. (a) Initial (b) After Ba-exchange (c) After heating to 850 °C for 2 h and (d) After heating to 1000 °C for 1 h and (e) After heating to 1200 °C for 28 h.

these differences changes in the ^{29}Si NMR spectra for X II with temperature are essentially identical to those seen for X I. Overall then the feature of the ^{29}Si NMR spectra is the remarkable similarity in the two sets of data. At the level of the short range ordering seen by solid state NMR the thermal transformations is highly reproducible.

4.2. *^{27}Al NMR*

Three aspects of a ^{27}Al NMR spectrum are of value in characterising the local environment of the ^{27}Al nucleus [25]. First, the central transition 1/2 to −1/2 which gives the isotropic chemical shift and any second-order quadrupolar

coupling contributions. Second, the satellite transitions, of which 3/2–1/2 is an example, which shows the first-order quadrupolar interaction and third, the linewidths of the transitions which are related, in part, to disorder within the sample. Quantitative data about the ^{27}Al quadrupolar coupling constants is difficult to obtain from the spinning sideband manifold in high Q MAS probes because of the limited nature of their bandwidth compared to the magnitude of the quadrupolar coupling constants [27]. Typically this shows up as the distorted intensities commonly seen for the spinning sidebands associated with the satellite transitions [28]. Despite the distortions, the shape of the spinning sideband manifold still gives excellent qualitative information about the nature of the quadrupolar coupling constant. If required the distortions can be corrected for, however, this was not necessary in the present case since the precise values of the quadrupolar coupling constant do not materially affect the analysis based on the ^{29}Si NMR. A clearer indication of the quadrupolar coupling constants can be obtained by MQ MAS NMR experiments, which also allow resonances with similar chemical shifts but differing quadrupolar parameters to be resolved [29].

The principal determinant of the ^{27}Al chemical shift is the co-ordination number with four co-ordinate around 60–80 ppm, five co-ordinate 20–40 ppm and six co-ordinate around -10 to $+10$ ppm [25]. The nature of the co-ordinated atoms, the bond angles and distances as well as the cations all modify the chemical shift within these ranges. In a crystalline material the presence of a unique set for these variables for each aluminium site means that the lines are narrow, except where residual dipolar coupling is present. However, in an amorphous material where the bond angles and distances can show a large variation even when the basic co-ordination unit remains, AlO_4 in this instance, results in broad lines. Tellingly the chemical shift is only able to identify structural units through a matching of chemical shifts, with the attendant problems of coincidence and poor resolution.

Previous work has shown that monoclinic and hexagonal celsian show clear differences in the appearance of the central and satellite transitions of their ^{27}Al MAS NMR spectrum [16]. Both having relatively narrow resonances consistent with a high degree of order. The hexagonal celsian is characterised by a single central transition resonance ($\delta = 60.7$ ppm, $\Delta\nu_{1/2} = 1$ kHz) consistent with the single aluminium site found in the crystal structure [24]. On the other hand the monoclinic form shows two resolvable resonances($\delta = 60.8$ and 57.3 ppm, $\Delta\nu_{1/2} = 1.6$ kHz), while the crystal structure shows four possible sites [30]. These chemical shifts represent a fingerprint for the structural units in celsian. The ^{27}Al MAS NMR spectrum of the starting zeolite Na-X shows a single central transition at 62.8 ppm ($\Delta\nu_{1/2} = 897$ Hz), while for (Na,K)-X two resonances are seen, one at 63.8 ppm ($\Delta\nu_{1/2} = 463$ Hz) and the other a shoulder at 59.5 ppm ($\Delta\nu_{1/2} = 669$ Hz). This shoulder is due to the presence of a small amount of zeolite A as evidenced by the XRD pattern (not reported). All the resonances are characteristic of tetrahedral aluminium (AlO_4). As seen previously both zeolites showed a weaker spinning sideband manifold in comparison with Na-A [16], than might have been expected on the basis of their similar quadrupolar coupling constants of ca 1.1 MHz owing to the increase in the chemical shift anisotropy.

On exchanging the sodium for barium in both X zeolites the resonance becomes more shielded and broadens somewhat, (X I: $\delta = 57.8$ ppm, $\Delta\nu_{1/2} = 830$ Hz; X II: $\delta = 56.7$ ppm, $\Delta\nu_{1/2} = 920$ Hz) indicative of a loss of local order. However, since the resonances remain rather narrow the material must still be ordered to some extent. Thus, in contrast to zeolite A [16] barium exchange has not disrupted the longer-range order in zeolite X. The minor variation seen in the isotropic chemical shift represents the effect of the change in cation to Ba^{2+} as well as the bond angles and distance. The fact only small differences were seen in the ^{27}Al chemical shift of aluminium in an AlO_4 environment is not uncommon in ^{27}Al NMR. Often the changes in chemical shift are barely discernible within the relatively broad central resonance. Increases in the linewidth of the central transition reflect an increase in the chemical shift distribution arising from short range disorder within the lattice corresponding to a range in local co-ordination geometries, both changes in the nearest neighbour bond lengths and bond angles as well as more distant next nearest neighbour influences.

Heating the Ba exchanged zeolites X I and II to 850 °C results in the collapse of the ordered zeolitic structure and the formation of amorphous glassy phases as shown by the broad resonance ($\Delta\nu_{1/2} \approx 3$ kHz) with the two zeolites having essentially the same ^{27}Al NMR spectrum, although there is a slight shift of the Ba-X spectrum to more shielded values. In addition the satellite transition manifold is more extensive. In line with the comments above, the increase in the resonance linewidth is explicable in terms of an increase in the chemical shift dispersion resulting from greater short-range disorder as the regular lattice of the zeolite is destroyed. Asymmetry of the central transition is observed on the more shielded side of the resonance, 30–40 ppm giving rise to intensity in a region normally associated with AlO_5 co-ordination. As noted previously the most likely explanation for this is a distribution of quadrupolar interactions, albeit reduced somewhat by the high static field, 14.07 T used to acquire the data rather than AlO_5 co-ordination. A related picture is shown by the satellite transitions, the greater spread in the manifold shows a larger quadrupolar coupling constant and hence electric field gradient at the nucleus. This in turn must reflect a greater distortion in the AlO_4 geometry from true tetrahedral. However, as with the Ba exchanged zeolite A it is not possible to comment on the range of distortions from a qualitative inspection of the satellite transitions. Close comparison of the appearance of the central transition in the ^{27}Al NMR spectrum of the Ba exchanged

zeolites X after heating to 850 °C and the earlier data on Ba-A after heating to 700 °C [16] indicates differences are present which suggest they do not describe a common precursor state. Although zeolites X I and II are similar, zeolite A differs in having a somewhat narrower component to the lineshape around 60 ppm which would be consistent with the hypothesis of the Ba-A material containing nuclei of monoclinic celsian. But precisely because of the difficulties in deducing structural features from the broad NMR spectrum it is not possible to say conclusively whether this is so.

Finally on heating the Ba-X I and II samples to 1000 and 1200 °C, the crystalline hexagonal celsian can be seen by the narrow ^{27}Al resonance at 60.3 ppm. In both cases the higher temperature used for the heat treatment led to a more ordered material and thus a narrower resonance. Also the presence of monoclinic celsian can be seen through the slight asymmetry in the central transition since the ^{27}Al resonance in the standard hexagonal phase is symmetrical while the monoclinic phase gave resonances which are more shielded at ca. 59 ppm.

5. Conclusions

The thermal transformations of two barium-exchanged zeolites X have been studied by ^{27}Al and ^{29}Si MAS NMR spectroscopy. Overall the ^{27}Al and ^{29}Si NMR spectra demonstrate a remarkable similarity. Only minor differences can be seen between the NMR spectra of the two X zeolites, starting from the initial barium exchange, through the spectra typical of amorphous materials seen on heating to 850 °C, to the high temperature formation of the mixture of hexagonal and monoclinic celsian. Thus the short range order present in the two barium exchanged zeolite X must be similar at each stage of the thermal treatment despite the differences in their Si/Al ratio. Excess silicon in both cases results in a non-stoichiometric celsian with some evidence for clustering of the substituting silicon. ^{27}Al NMR spectra lend weight to the hypothesis that more ordered nuclei of monoclinic celsian are present in Ba-A than Ba-X.

Acknowledgments

This work was carried out with the financial contribution of the MIUR (Ministero dell'Istruzione, dell'Università e della Ricerca). We thank Dr. A. Howes, Department of Physics, University of Warwick for the 14.07 T ^{27}Al MAS NMR spectra.

Appendix A. Supplementary Materials

Supplementary data associated with this article can be found in the online version at doi:10.1016/j.jssc.2006.03.021.

References

[1] M.A. Subramanian, D.R. Corbin, R.D. Farlee, Mat. Res. Bull. 21 (1986) 1525–1532.
[2] U.V. Chowdry, D.R. Corbin, M.A. Subramanian, US Patent 4,813,303, March 21, 1989.
[3] M.A. Subramanian, D.R. Corbin, U.V. Chowdry, Adv. Ceram. 26 (1989) 239–247.
[4] D.R. Corbin, J.B. Parise, U.V. Chowdry, M.A. Subramanian, Mater. Res. Symp. Proc. 233 (1991) 213–217.
[5] D.S. Coombs, A. Alberti, T. Ambruster, G. Artioli, C. Colella, E. Galli, J.D. Grice, F. Liebau, J.A. Mandarino, H. Minato, E.H. Nickel, E. Passaglia, D.R. Peacor, S. Quartieri, R. Rinaldi, M. Ross, R.A. Sheppard, E. Tillmanns, G. Vezzalini, Can. Mineralogist 35 (1997) 1571–1606.
[6] C. Baerlocher, W.M. Meier, D.H. Olson, Atlas of the Zeolite Framework Types, Elsevier, Amsterdam, 2001.
[7] D.W. Breck, Zeolite Molecular Sieves: Structure, Chemistry and Use, Wiley, New York, 1974.
[8] B. Hoghooghi, J. McKittrick, C. Butler, Mater. Res. Soc. Symp. Proc. 348 (1994) 493–498.
[9] B. Hoghooghi, J. McKittrick, C. Butler, P. Desch, J. Non-Cryst. Sol. 170 (1994) 303–307.
[10] J. McKittrick, B. Hoghooghi, O.A. Lopez, J. Non-Cryst. Sol. 197 (1996) 170–178.
[11] B. Hoghooghi, J. McKittrick, E. Helsel, O.A. Lopez, J. Am. Ceram. Soc. 81 (4) (1998) 845–852.
[12] A. Ata, B. Hoghooghi, J. McKittrick, E. Helsel, J. Loam, J. Mater. Symp. Proc. 5 (3) (1997) 217–225.
[13] G. Dell'Agli, C. Ferone, M.C. Mascolo, M Pansini, Solid State Ionics 127 (2000) 309–317.
[14] C. Ferone, G. Dell'Agli, M.C. Mascolo, M Pansini, Chem. Mater. 14 (2002) 797–803.
[15] A. Aronne, S. Esposito, C. Ferone, M. Pansini, P. Pernice, J. Mater. Chem. 12 (2002) 3039–3045.
[16] N.J. Clayden, S. Esposito, C. Ferone, M. Pansini, J. Mater. Chem. 13 (2003) 1681–1685.
[17] S. Esposito, C. Ferone, M. Pansini, L. Bonaccorsi, E. Proverbio, J. Eur. Ceram. Soc. 24 (2004) 2689–2697.
[18] I.G. Talmy, D.A. Haught, E.J. Wuchina, in: A.B. Goldberg, C.A. Harper (Eds.), in: Proceedings of the 6th International SAMPE Electronic Conference, Society for the Advancement of Materials and Process Engineering, Covina, CA USA, 1992, p. 687.
[19] C.H. Drummond III, J. Non-Cryst. Solids 123 (1990) 114–128.
[20] V. Dondur, R. Dimitrijevic, A. Kremenovic, U.B. Mioc, R. Srejic, M. Tomasevic-Canovic, in: P. Vincenzini (Ed.), Advances in Science and Technology, vol. 3, part B, Techna, Faenza, 1995, p. 687.
[21] R. Dimitrijevic, V. Dondur, A. Kremenovic, Zeolites 16 (1996) 294–300.
[22] M.G. Skellern, R.A. Howie, E.E. Lachowski, J.M.S. Skakle, Acta Cryst. C 59 (2003) i11.
[23] A.J. Vega, ACS Symp. Ser. 218 (1983) 217–230.
[24] A. Kremenovic, P. Norby, R. Dimitrijevic, V. Dondur, Solid State Ionics 101 (1997) 611–618.
[25] G. Engelhardt, D. Michel, High Resolution Solid-State NMR of Silicates and Zeolites, Wiley, Chichester, 1987.
[26] J. Djordjevic, V. Dondur, R. Dimitrijevic, A. Kremenovic, Phys. Chem. Chem. Phys. 3 (2001) 1560–1565.
[27] G. Kunath-Fandrei, T.J. Bastow, J.S. Hall, C. Jäger, M.E. Smith, J. Phys. Chem. 99 (1995) 15138–15141.
[28] J. Skibsted, N.C. Nielsen, H. Bildsøe, H.J. Jacobsen, J. Magn. Reson. 95 (1991) 88.
[29] L. Frydman, J.S. Harwood, J. Am. Chem. Soc. 117 (1995) 5367.
[30] D.T. Griffen, P.H. Ribbe, Am. Mineral. 61 (1976) 414–418.